doi:10.1093/brain/awn222 *Brain* (2008), **131**, 2679–2689

ABCC1: a gateway for pharmacological compounds to the ischaemic brain

Ertugrul Kilic,[1] Annett Spudich,[1] Ülkan Kilic,[1] Katharina M. Rentsch,[2] Raluca Vig,[1] Christian M. Matter,[3] Heidi Wunderli-Allenspach,[4] Jean-Marc Fritschy,[5] Claudio L. Bassetti[1] and Dirk M. Hermann[1]

[1]Department of Neurology, [2]Department of Clinical Chemistry, [3]Department of Cardiology, University Hospital Zurich, Frauenklinikstr. 26, CH-8091 Zurich, [4]Institute of Pharmaceutical Sciences, Swiss Federal Institute of Technology, Wolfgang-Pauli-Str. 10, CH-8093 Zurich and [5]Institute of Pharmacology and Toxicology, University of Zurich, Winterthurer Str. 190, CH-8057 Zurich, Switzerland

Correspondence to: Prof. Dr. Dirk M. Hermann, Department of Neurology, University of Duisburg-Essen, Hufelandstr. 55, D-45122 Essen, Germany
E-mail: dirk.hermann@uk-essen.de

By preventing access of drugs to the CNS, the blood–brain barrier hampers developments in brain pharmacotherapy. Strong efforts are currently being made to identify drugs that accumulate more efficaciously in ischaemic brain tissue. We identified an ATP-binding cassette (ABC) transporter, ABCC1, which is expressed on the abluminal surface of the brain capillary endothelium and mildly downregulated in response to focal cerebral ischaemia, induced by intraluminal middle cerebral artery occlusion. In biodistribution studies we show that ABCC1 promotes the accumulation of known neuroprotective and neurotoxic compounds in the ischaemic and non-ischaemic brain, ABCC1 deactivation reducing tissue concentrations by up to two orders of magnitude. As such, ABCC1's expression and functionality in the brain differs from the liver, spleen and testis, where ABCC1 is strongly expressed on parenchymal cells, resulting—in case of liver and testis—in directed transport from the tissue into the blood. After focal cerebral ischaemia, ABCC1 deactivation abolished the efficacy of both neuroprotective and neurotoxic compounds. Our data indicate that ABCC1 acts as gateway for pharmacological compounds to the stroke brain. We suggest that the tailoring of compounds binding to abluminal but not luminal ABC transporters may facilitate stroke pharmacotherapy.

Keywords: ABC transporter; blood–brain barrier; neuroprotection; pharmacotherapy; stroke

Abbreviations: ABC = ATP-binding cassette; BBB = blood–brain barrier; LC-MS = liquid chromatography/mass spectrometry; LDF = laser Doppler flow; MCA = middle cerebral artery; Mdr = multi-drug resistance transporter; Mrp = multi-drug resistance-associated protein; TUNEL = terminal transferase biotinylated-dUTP nick end labelling

Received February 12, 2008. Revised August 11, 2008. Accepted August 22, 2008. Advance Access publication September 16, 2008

Introduction

Pharmacological therapies have made limited progress in the brain recently (Löscher and Potschka, 2005; Hermann *et al.*, 2006). As such, many candidate drugs evaluated in clinical trials have failed, particularly in ischaemic stroke (O'Collins *et al.*, 2006; Hermann and Bassetti, 2007). A major obstacle for newly developed compounds is the blood–brain barrier (BBB), which prevents systemically administered molecules from entering the brain (Pardridge, 2002; Begley, 2004). The BBB acts not only as passive diffusion barrier. It expresses active transporters that eliminate drugs from the brain tissue (Löscher and Potschka, 2005; Hermann *et al.*, 2006).

Strong efforts have been made in recent years to identify pharmacological compounds that accumulate more efficaciously in the diseased brain. As such, the physicochemical properties of compounds (e.g. lipophilicity, surface charges, molecular size), their uptake via receptor-dependent or -independent endocytosis, as well as their binding to membrane-bound ATP-binding cassette (ABC) transporters and solute carriers were recognized to influence drug accumulation (Begley, 2004; Hermann *et al.*, 2006).

In contrast to solute carriers, which are bi-directional, low-affinity transporters driven by concentration gradients of endogenous molecules (e.g. carnithine, urate, Na^+, H^+), carrying organic compounds through cell membranes both in an inward and outward direction (Meier and Stieger, 2002; Hagenbuch and Meier, 2004), ABC transporters are unidirectional high-affinity pumps eliminating a broad

variety of chemically unrelated lipophilic and amphipathic molecules from cells in an ATP-dependent manner (Higgins *et al.*, 1986; Löscher and Potschka, 2005), among which there are many pharmacological compounds.

ABC transporters have received considerable interest in the brain recently, since they impede the brain accumulation of drugs. In fact, most ABC transporters, such as their best-characterized member ABCB1 [previously called multi-drug resistance transporter (Mdr)-1], are abundantly expressed on the luminal membrane of brain capillary cells (Löscher and Potschka, 2005; Hermann and Bassetti, 2007). As a consequence, these transporters extrude drugs from the brain back into the blood (Rizzi *et al.*, 2002; Löscher and Potschka, 2005; Spudich *et al.*, 2006).

Not all ABC transporters exhibit luminal endothelial expression. For the transporter ABCC1 [formerly multi-drug resistance-associated protein (Mrp)-1], it was recently demonstrated that this transporter is predominantly expressed on the abluminal endothelial membrane (Soontornmalai *et al.*, 2006). Similar to ABCB1, ABCC1 reveals strong binding affinity to many amphipathic compounds (Hermann and Bassetti, 2007). Besides, ABCC1 also binds glucuronidated, glutathionized and sulphated molecules, which are not ABCB1 substrates (Hermann and Bassetti, 2007).

Until now, the relevancy of ABCC1 for pharmacological therapies remained unknown. Using immunohistochemical studies, Western blots with capillary-enriched brain tissue fractions and experiments, in which we deactivated ABCC1 by pharmacological inhibition or genetic knockout, we now examined the role of ABCC1 in the ischaemic brain, analysing its effect on drug accumulation and efficacy after middle cerebral artery (MCA) occlusion.

Methods

Focal cerebral ischaemia

Experiments were performed in accordance to National Institutes of Health (NIH) guidelines for the care and use of laboratory animals and approved by local government authorities (Kantonales Veterinäramt; ZH169/2005). Male C57Bl6/j mice as well as male *abcc1*$^{-/-}$ mice, produced on a FVB.129P2 background (Taconic, New York, USA) together with *abcc1*$^{+/+}$ controls, were used. At the age of 8–10 weeks (animal weight: 20–23 g), animals were anaesthetized with 1% isoflurane (30% O_2, remainder N_2O). Rectal temperature was maintained between 36.5°C and 37.0°C, and laser Doppler flow (LDF) was monitored with a flexible fiberoptic probe that was placed above the core of the MCA territory (Perimed, Stockholm, Sweden) (Wang *et al.*, 2005; Kilic *et al.*, 2006). Focal cerebral ischaemia was induced by intraluminal MCA occlusion, as previously described (Wang *et al.*, 2005; Kilic *et al.*, 2006). Sham animals received neck incisions, in which the common carotid artery was isolated, but not ligated or cut. At indicated times (specified below), in case of sham animals after 3 h reperfusion, animals were re-anaesthetized and transcardially perfused with normal saline [immunohistochemistry/Western blots; liquid chromatography/mass spectrometry (LC-MS) for the ABCC1 substrate 17β-estradiol-17β-D-glucuronide (17βEG)] or killed by decapitation [LC-MS for the ABCC1 substrate *S*-nitrosoglutathione (GSNO); drug-efficacy studies]. Brains, liver, spleen and testis were removed, frozen and cut into coronal 18 µm cryostat sections for immunohistochemistry of ABC transporters, terminal transferase biotinylated-dUTP nick end labelling (TUNEL) or cresyl violet staining. Tissue samples were also taken from both MCA territories (lateral parietal cortex and underlying striatum), the liver, spleen and testis for Western blots and LC-MS.

Immunohistochemistry for ABCC1 and other multi-drug transporters

Cryostat sections from mice submitted to sham surgery (3 h survival) or to 30 or 90 min of MCA occlusion (3 h reperfusion) ($n = 5$ animals per group) were fixed in 4% paraformaldehyde in 0.1 M phosphate-buffered saline (PBS), blocked in 0.1 M PBS containing 0.3% Triton-X-100 (PBS-T) and 10% normal goat serum (NGS) and incubated overnight at 4°C with polyclonal guinea pig anti-mouse ABCC1 (clone J95 ESD8; Institute of Pharmacology and Toxicology, University of Zurich), polyclonal rabbit anti-human ABCB1 (H-241, sc-8313; Santa Cruz Biotechnology, Santa Cruz, CA, USA), polyclonal rabbit anti-mouse ABCC2 (clone J81 ESD2; Institute of Pharmacology and Toxicology), polyclonal rabbit anti-rat ABCC3 (clone J81 ESD3; Institute of Pharmacology and Toxicology) or monoclonal rat anti-human ABCC5 (ALX801021-C250 or ALX801022-C250; Alexis, Lausen, Switzerland) antibody, diluted 1 : 100 in 0.1 *M* PBS-T containing 2% NGS. Sections were counterlabelled with rat or goat anti-CD31 (BD Biosciences, Basle, Switzerland), mouse anti-NeuN (MAB377; Chemicon, Lucerne, Switzerland) or rabbit anti-GFAP (Dako, Zug, Switzerland) antibody. The specificity of the ABCC1, ABCB1, ABCC2, ABCC3 and ABCC5 antibodies in the brain has previously been shown (Soontornmalai *et al.*, 2006; Spudich *et al.*, 2006). In fact, negative controls, in which antibodies were omitted, did not result in any staining (data not shown). As positive controls, liver and kidney sections were used (Soontornmalai *et al.*, 2006). Sections were evaluated microscopically by a blinded investigator. ABCC1 expression levels were evaluated by counting densities of ABCC1+ capillaries in a total of six rectangular random regions of interest (ROI) in the ischaemic and non-ischaemic striatum, each 1 mm apart, and additional six random ROI in the parietal cortex, 600 µm apart, each ROI measuring 62 500 µm^2 (Spudich *et al.*, 2006).

Western blots for ABCC1

Ten micrograms of enriched microvessel protein (for preparation see Spudich *et al.*, 2006) obtained from pooled tissue samples of C57Bl6/j mice submitted to sham surgery (3 h survival), 30 min (3, 24 or 72 h reperfusion) or 90 min (3, 12 or 24 h reperfusion) of MCA occlusion ($n = 5$ animals per group) were subjected to sodium dodecylsulphate–polyacrylamide gel electrophoresis (SDS–PAGE) and transferred onto polyvinylidene fluoride (PVDF) membranes. After blocking, membranes were incubated in a monoclonal rat antibody that specifically recognizes ABCC1 (ALX801007, Alexis; diluted 1:100 in 0.1% TBS-T containing 5% milk). Following incubation in peroxidase-coupled secondary antibody, membranes were immersed in enhanced chemoluminescence (ECL) solution and exposed to ECL-Hyperfilm (Amersham, Otelfingen, Switzerland). Protein loading was controlled with a mouse anti-β-actin antibody (Sigma-Aldrich). Blots revealed a ~190 kDa band that was absent in control studies in which the primary antibody was omitted. Blots were digitized, ABCC1 levels

densitometrically analysed, corrected for protein loading and expressed as relative values compared with ABCC1 levels in sham-operated mice.

Effects of ABCC1 inhibition on the brain accumulation of 17βEG and GSNO

To evaluate how ABCC1 deactivation affects drug accumulation in the brain, we used a pharmacological inhibition strategy using MK571 (Alexis, Lausen, Switzerland), a potent ABCC1 blocker (Kimura *et al.*, 2005). Two different ABCC1 substrates were assessed, namely 17βEG (Sigma-Aldrich) (Cisternino *et al.*, 2003) and GSNO (WPI Europe, Berlin, Germany) (Khan *et al.*, 2005). To evaluate drug accumulation in the brain, C57Bl6/j mice submitted to 30 min MCA occlusion were treated via the femoral vein with either vehicle (0.9% NaCl) or MK571 (10 mg kg^{-1} body weight, dissolved in 0.9% NaCl), 60 min later followed by 17βEG (10 mg kg^{-1}, in 0.9% NaCl) ($n = 5$–7 animals per group) or GSNO (1 mg kg^{-1}, in 0.9% NaCl) ($n = 4$ animals per group). Two hours (in case of 17βEG) or 2 min (in case of GSNO) later, blood samples were collected in vials coated with lithium heparinate (Vacutainer; Becton Dickinson, Basle, Switzerland) and animals were sacrificed. The time point of 2 min in case of GSNO was chosen in view of the high instability of this NO donor. In a first set of studies, in which animals were killed 15 min or 2 h after GSNO infusion, brain levels have been close to or even below detection limits (data not shown). In the plasma and brain samples obtained, 17βEG, its deglucuronidated parent compound 17β-estradiol (17βE) and GSNO were analysed by LC-MS. Similarly, 17βEG and 17βE levels were determined by LC-MS in the animals' liver, spleen and testis.

LC-MS for 17βEG and 17βE

Weighted tissue samples were homogenized in 0.9% NaCl and divided into three portions as follows: In portion 1, the concentration of 17βE was quantified by the addition of 2.5 pmol 17βE-d3 (Sigma-Aldrich) in 50 µl 90% (v/v) ethanol and 50 µl phosphate buffer (50 mM, pH 7.0). After extraction with 3 ml dichloromethane, separation of the organic phase and evaporation of the solvent, 17βE and 17βE-d3 in the residue was derivatized by adding 50 µl carbonate buffer (100 mM, pH 10.5) and 50 µl dansyl chloride in acetone (1 mg ml^{-1}) for 3 min at 60°C. After cooling to room temperature, the solution was directly injected into the high-performance liquid chromatography (HPLC) system. In portion 2, the total amount of 17βE and 17βEG was quantified by the addition of 2.5 pmol 17βE-d3 in 90% (v/v) ethanol and 50 µl (1000 U) β-glucuronidase (Sigma-Aldrich) in phosphate buffer. The deglucuronidation was performed for 1 h at 37°C. In portion 3, 2.5 pmol 17βE in 50 µl phosphate buffer pH 7.0 and 2.5 pmol 17βEG-d3 in 90% (v/v) ethanol were added to enable tissue quantification of 17βE. The extraction and derivatization in portions 2 and 3 were identical as described for portion 1. The extraction and derivatization of plasma was identical as that for tissue samples. For analysis, 50 µl plasma were complemented with 2.5 pmol 17βE-d3 in 50 µl 90% (v/v) ethanol, 50 µl phosphate buffer pH 7.0 and 200 µl 0.9% NaCl.

The dansylated 17βE was analysed by the LC-MS/MS system consisting of a Rheos 2000 pump (Flux Instruments, Basle, Switzerland), a PAL autosampler (CTC Analytics, Zwingen, Switzerland) and a LCQ TSQ 7000 (ThermoQuest, San Jose, CA, USA) using selected reaction monitoring. An Uptisphere 5 ODB column (125 × 2 mm; Interchim, Montluçon, France) was used. The mobile phase was a gradient of water/acetonitrile (95/5, v/v) against water/acetronitrile/methanol (5/30/65, v/v) containing 0.1% formic acid. The flow rate was also run as a gradient between 0.2 and 0.3 ml min^{-1}. The ionization mode was positive atmospheric pressure chemical ionization. The vaporizer temperature and capillary temperature were kept at 450°C and 250°C, respectively, the discharge current fixed at 6 µA. The sheath gas pressure was held at 60 psi, the auxiliary gas pressure at 15 psi, respectively. The tissue concentration of 17βE was calculated using the standard addition method. Standard curves for 17βE in plasma were linear with a correlation coefficient of <0.999 and the coefficients of variations <6%. With the concentrations determined, tissue-to-plasma concentration ratios were calculated, which were expressed—unless otherwise specified—as pmol g^{-1} (tissue) per pmol $µl^{-1}$ (plasma).

LC-MS for GSNO

Weighted tissue samples were homogenized with 30 mM ammonium sulphamate in 0.9% NaCl solution containing 0.4% sodium fluoride. To brain homogenates and plasma samples, ammonium sulphamate (30 mM) in 0.9% NaCl was added to remove endogenous nitrite. One-hundred picomole [^{15}N]-GSNO, synthesized by *S*-nitrosylation of GSH with acidified [^{15}N]-$NaNO_2$ (Dr Glaser, Basle, Switzerland), was used as internal standard. Proteins were precipitated with 30 mM ammonium sulphamate and 10% trichloroacetic acid (TCA) in water and the precipitate was centrifuged at 20 000*g* for 10 min at 5°C. The supernatants were neutralized with 4 M dipotassium hydrogenphosphate to pH 6.0, mixed with 1 M borate buffer to final pH 7.5-8.0 and derivatized for 1 min with 15.5 mM 9-fluorenylmethyl chloroformate (FMOCCl; Fluka, Buchs, Switzerland) in acetone at room temperature. The excess of FMOCCl was removed by extracting with 2 ml *n*-pentane.

The FMOC-GSNO in the aqueous phase was analysed by the LC-MS/MS system (analytical instrumentation as above) under an elution gradient of water/acetonitrile (95/5, v/v) containing 0.1% formic acid against water/acetronitrile/methanol (5/30/65, v/v) containing 0.1% formic acid. The flow rate was 0.3 ml min^{-1}. The capillary temperature was kept at 250°C, the electrospray voltage at 5 kV (negative ionization). The sheath gas pressure was held at 60 psi, the collision gas (argon) pressure at 1.30 mTorr, respectively. Standard curves for GSNO in plasma were linear with a correlation coefficient of <0.999. Coefficients of variation for the LC-MS assay were <6%. The concentrations of GSNO in brain homogenates were determined using the standard addition method. Tissue-to-plasma concentration ratios were calculated and expressed as pmol g^{-1} (tissue) per pmol $µl^{-1}$ (plasma).

Effects of ABCC1 deactivation on ischaemic brain injury

The protocol of the drug efficacy studies is summarized in Supplementary Fig. 1. Two different ABCC1 deactivation strategies were used in mice subjected to 30 or 90 min MCA occlusion, namely pharmacological inhibition with MK571 and genetic *abcc1*$^{-/-}$. Animals undergoing 30 min MCA occlusion were intraperitoneally treated with vehicle (0.9% NaCl) or MK571 (10 mg kg^{-1} body weight, as above) immediately after reperfusion and at 24 and 48 h after stroke. Always 60 min later, either vehicle (0.9% NaCl), 17βEG (2, 5, 10 or 50 mg kg^{-1} body weight, as above) or GSNO (0.2, 0.5, 1 or 5 mg kg^{-1} body weight, as above) were intraperitoneally applied ($n = 7$–8 animals per group).

Animals were sacrificed 72 h after reperfusion onset. Mice subjected to 90 min of MCA occlusion were intraperitoneally treated with either vehicle or MK571 (10 mg kg^{-1} body weight, as above) immediately after reperfusion, 10 min later followed by vehicle, 17βEG (2 or 10 mg kg^{-1} body weight, as above) or GSNO (0.2 or 1 mg kg^{-1} body weight, as above) ($n = 6$–8 animals per group). These animals were killed 24 h following stroke.

Analysis of histological brain injury

Brain sections from the level of the mid-striatum (bregma 0.0 mm) of animals submitted to 30 min MCA occlusion were fixed with 4% paraformaldehyde in 0.1 M PBS and stained by TUNEL using a commercially available kit (Roche, Basle, Switzerland). In these sections, DNA fragmented cells were counted in blinded manner in six random ROI in the striatum (1 mm apart), and six random ROI in the cortex (600 µm apart), each measuring 62 500 μm^2. These ROI were chosen as 30 min MCA occlusion usually leads to disseminate neuronal damage in the mouse striatum (Wang *et al.*, 2005; Spudich *et al.*, 2006), which may expand into the cortex under conditions of exacerbated brain injury. In fact, exclusively striatal DNA fragmentation was seen in our present studies in case of most vehicle-treated or 17βEG-treated animals, whereas GSNO delivered at doses of 1 or 5 mg kg^{-1} reproducibly resulted also in cortical cell death. Animals subjected to 90 min MCA occlusion were analysed by staining a total of four sections from equidistant brain levels, 2 mm apart (starting from the rostral pole of the striatum: bregma +2.0 mm, followed by sections at levels bregma 0.0, –2.0 and –4.0 mm) with cresyl violet. Brain infarcts were outlined on these sections by delineating non-lesioned tissue in both hemispheres, thereby determining oedema-corrected infarct areas, and subsequently calculating infarct volumes (Wang *et al.*, 2005; Kilic *et al.*, 2006).

Statistics

Results are presented as means ± SD. Data were analysed by one-way ANOVA followed by least significant differences (LSD) tests (comparisons between ⩾3 independent groups), repeated measurement ANOVA (comparisons between ⩾4 groups including within-subject comparisons), two-way ANOVA (comparisons between four independent groups elucidating drug interactions) or unpaired two-tailed *t*-tests (comparisons between two groups), using SPSS for Windows 12.0.1. In case of multiple comparisons being made, significance levels were adapted using Bonferroni corrections. *P*-values < 0.05 were considered significant.

Results

Distribution of ABCC1 in the brain and in peripheral tissues

In immunohistochemistries we observed that ABCC1 is expressed on the brain capillary endothelium of C57Bl6/j and FVB mice, where ABCC1 was almost exclusively found on the abluminal surface (Fig. 1). On the other hand, ABCC1 was undetectable on neurons or glial cells throughout the brain (Fig. 1). Thus, ABCC1 expression in the brain differed from peripheral tissues, where ABCC1 immunoreactivity was noticed on parenchymal cells and—in case of spleen and testis—vascular staining was faint (Fig. 2).

In the brain, ABCC1 levels were mildly reduced in response to focal cerebral ischaemia (Fig. 1). Western blots using enriched brain microvessel fractions revealed that ABCC1 expression decreased at 3 h and partly recovered within 24 to 72 h after stroke (Fig. 3).

Effect of ABCC1 inhibition on tissue accumulation of 17βEG and GSNO

To analyse how ABCC1 influences drug accumulation after stroke, we blocked ABCC1 in C57Bl6/j mice with MK571 (10 mg kg^{-1}) and concomitantly delivered the ABCC1 substrates 17βEG (10 mg kg^{-1}) or GSNO (1 mg kg^{-1}). Notably, ABCC1 deactivation decreased the brain-to-plasma concentration ratio of 17βEG and GSNO both in the ischaemic and non-ischaemic tissue by more than two orders of magnitude ($P < 0.001$; Fig. 4), as shown by LC-MS.

Following 17βEG delivery, the brain content not only of 17βE's 17β-D-glucuronide, but also its deglucuronidated parent compound 17βE was reduced (Fig. 4, $P < 0.05$), as our LC-MS studies revealed.

ABCC1's transport function in the brain differed from the liver and testis, where ABCC1 deactivation mildly increased 17βEG and—in case of liver—also 17βE levels ($P < 0.05$; Table 1). In the spleen, 17βEG and 17βE levels were not influenced by MK571 (Table 1).

Blood levels of 17βEG and GSNO remained unchanged after ABCC1 deactivation (Fig. 4). Blood levels of 17βE were low in both groups {log10[concentration(pmol ml^{-1})]: 0.32 ± 0.62 versus 1.10 ± 1.32 in vehicle versus MK571-treated mice}.

Effect of ABCC1 inhibition on survival effects of 17βEG and GSNO

To clarify whether ABCC1 inhibition attenuates the survival effects of 17βEG and GSNO, we again deactivated ABCC1 in ischaemic C57Bl6/j mice with MK571 and subsequently applied both drugs at various dosages. Experiments in animals submitted to 30 or 90 min MCA occlusion consistently showed attenuation both of 17βEG neuroprotection and GSNO neurotoxicity following ABCC1 blockade (Figs 5 and 6). As such, drug effects were almost abolished even at doses 10 times above the therapeutic threshold (Figs 5 and 6).

To evaluate the specificity of our pharmacological observations, we subsequently examined the effects of 17βEG and GSNO in *abcc1*$^{-/-}$ mice produced on a FVB background. Blunted drug responses in *abcc1*$^{-/-}$ as compared with *abcc1*$^{+/+}$ animals confirmed that the changes noticed after pharmacological transporter blockade were indeed linked to ABCC1 (Fig. 5).

In *abcc1*$^{-/-}$ mice, expression patterns of ABCB1, ABCC2, ABCC3 and ABCC5 were identical to *abcc1*$^{+/+}$ animals. Thus, ABCC2 and ABCC3, which also bind glucuronidated and/or glutathionized compounds (Löscher and Potschka, 2005), were absent and ABCB1 and ABCC5, which bind

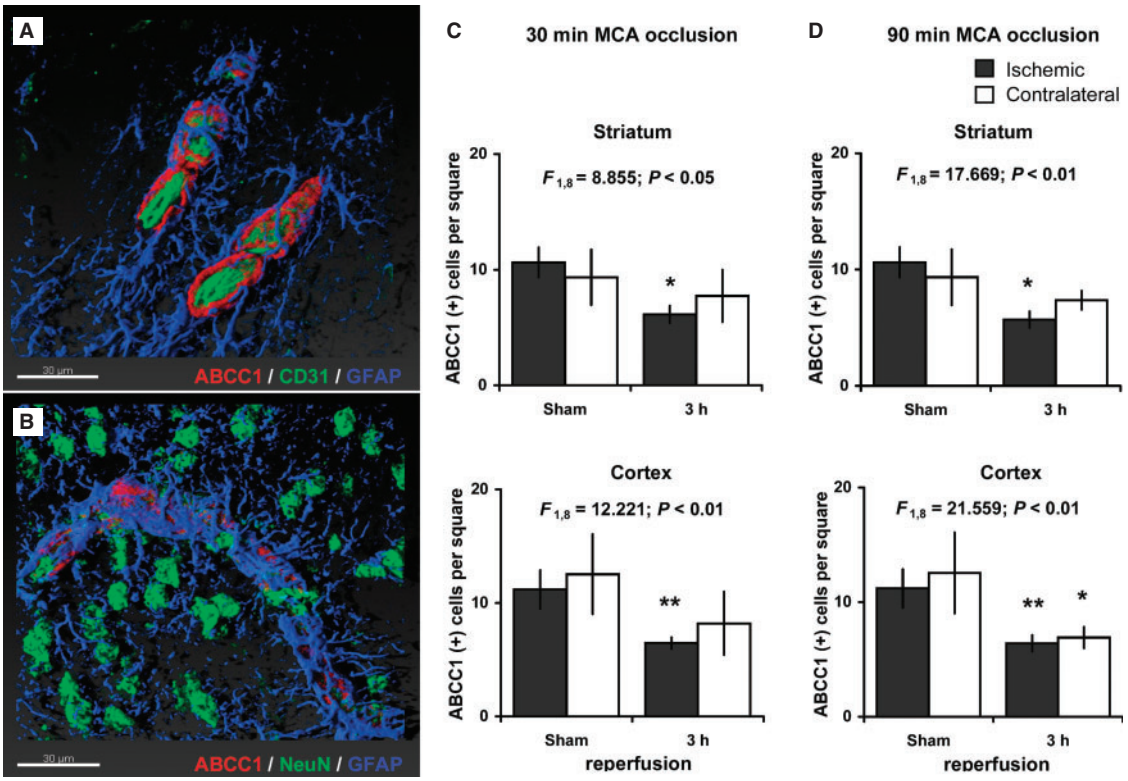

Fig. 1 ABCC1 is expressed on brain capillaries on the abluminal surface between the luminal membrane (CD31) and astrocytic endfeet (GFAP). Confocal laser scanning microphotographs showing ABCC1 in ischaemic vessels 3 h after 30 min MCA occlusion (**A** and **B**). Note the absence of ABCC1 in the brain parenchyma, i.e. on neurons (NeuN) and astrocytes (GFAP). The quantitative analysis of vessel densities in the cortex and striatum of mice submitted to 30 min (**C**) and 90 min (**D**) MCA occlusion reveals reduced ABCC1 levels at 3 h following stroke. Data from C57Bl6/j mice are shown. Data are means ± SD ($n = 5$ per group, repeated measurement ANOVA, time effects are shown, and *t*-tests). $^{*}P < 0.05$/$^{**}P < 0.01$ compared with contralateral sham. Bar = 30 μm.

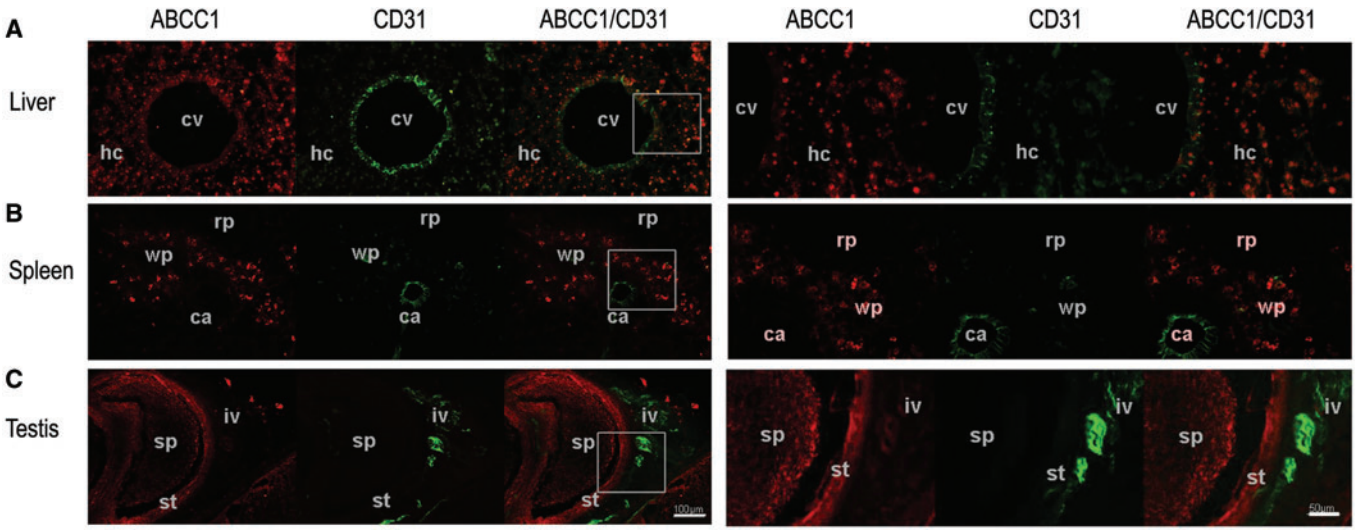

Fig. 2 ABCC1 distribution in the liver, spleen and testis differs from the brain. Immunohistochemistries revealing abundant ABCC1 expression (**A**) in the liver on CD31— hepatocytes (hc) and—slightly less intense—on endothelial cells of a central vein (cv), (**B**) in the spleen on CD31— cells of the white pulp (wp), but not on CD31+ central arteries (ca) and CD31— red pulp (rp), and (**C**) in the testis on spermatids (sp) and seminiferous tubules (st). Sections from C57Bl6/j mice are shown. Bar = 100 μm (left)/50 μm (right).

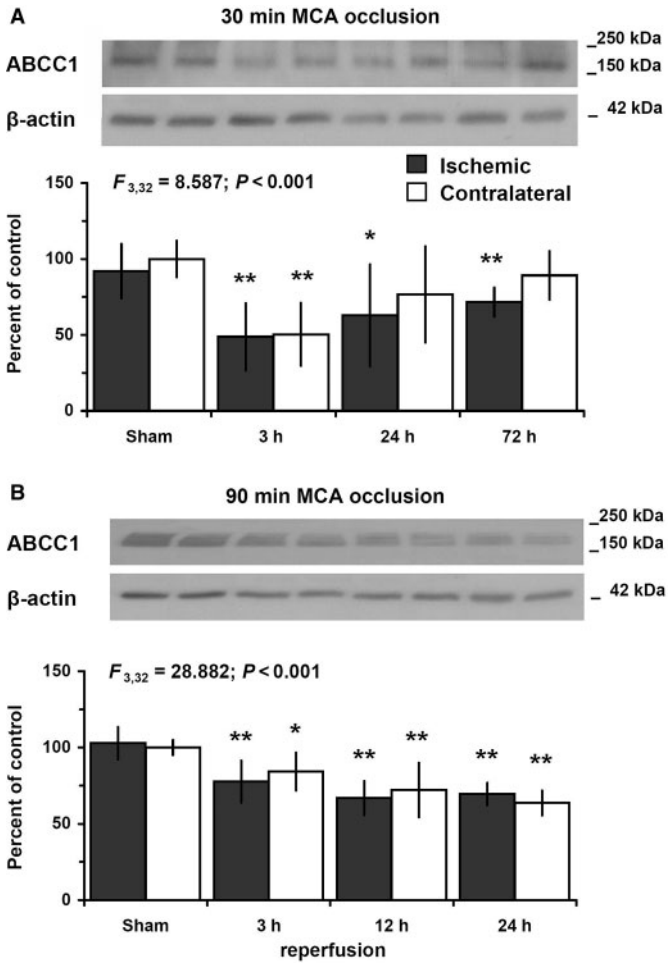

Fig. 3 ABCC1 expression decreases in response to focal cerebral ischaemia. Western blot analysis exhibiting the ~190 kDa ABCC1 protein in enriched microvessel fractions of brains from sham-animals and animals submitted to 30 min (**A**) or 90 min (**B**) MCA occlusion, followed by 3–72 h reperfusion. Note that ABCC1 levels declines already 3 h after ischaemia both in ischaemic and contralateral injury-remote tissue, recovering partly within 72 h after 30 min MCA occlusion. Data were analysed densitometrically and corrected for protein loading assessed on β-actin blots. Control experiments, in which the primary antibody was omitted, did not reveal any signal (data not shown). Capillary extracts from C57Bl6/j mice were used. Values are means ± SD ($n = 3$ different blots per group). Data were evaluated by repeated measurement ANOVA (time effects shown) and *t*-tests. $^{*}P < 0.05$/$^{**}P < 0.01$ compared with contralateral sham.

unconjugated but not conjugated molecules (Löscher and Potschka, 2005), were expressed at similar levels in both mouse lines (Supplementary Fig. 2).

Discussion

While the role of ABC transporters in drug elimination is well established in many diseases, including stroke, epilepsy and brain cancer (Löscher and Potschka, 2005; Hermann *et al.*, 2006), we for the first time provide evidence that an ABC transporter, ABCC1, actively promotes the accumulation and efficacy of pharmacological compounds in the ischaemic brain. As such, the profoundly reduced tissue levels, which were more than 100-fold below control conditions when ABCC1 was deactivated, suggest that drug accumulation may be more strongly than previously thought an active process. As ABCC1 is a broad-spectrum transporter, which binds a large variety of chemically unrelated substrates (Hermann and Bassetti, 2007), ABCC1 might offer itself as vehicle for drug delivery purposes. It is noteworthy that ABCC1 was still functional in the brain after ischaemia, despite the fact that ABCC1 levels were mildly reduced. ABCC1's retained functionality exemplifies its importance for drug biodistribution processes.

Transport activity attributed to expression pattern

ABCC1's role at the BBB profoundly differs from the liver, spleen and testis. In the liver and testis, ABCC1 deactivation mildly increased levels of the ABCC1 substrate 17βEG, just opposite to our findings in the brain. The specificities of pharmacological transport are attributed to differences in ABCC1 expression. As such, the abluminal endothelial expression of ABCC1 at the polarized BBB explains why the transporter promotes molecular uptake into the brain. On the other hand, parenchymal expression provides a rationale for ABCC1's role in drug removal in peripheral tissues. On the cellular level, ABC transporters act as ATP-dependent efflux pumps carrying drugs from the intracellular towards extra-cellular space. This directional transport was recently confirmed using crystal structures of ABC transporter molecules (Murakami *et al.*, 2006). It was also shown for ABCC1 in *in vitro* studies, in which ABCC1 was deactivated by pharmacological blockade, small-interfering RNA or genetic knockout (Regina *et al.*, 1998; Seetharaman *et al.*, 1998; Müller *et al.*, 2005).

ABCC1 expression in the brain had been a matter of debate previously. *In vitro* studies with rodent, bovine and human brain microvessels reported ABCC1 expression on endothelial cells and astrocytes (Regina *et al.*, 1998; Seetharaman *et al.*, 1998; Berezowski *et al.*, 2004). Importantly, ABCC1 levels increased with cell culturing, suggesting that its role *in vivo* differs from *in vitro* (Regina *et al.*, 1998; Seetharaman *et al.*, 1998). ABCC1 has been observed on astrocytes in models of drug-refractory epilepsy (Dombrowski *et al.*, 2001; van Vliet *et al.*, 2005). In drug-refractory epilepsy, several ABC transporters are induced (van Vliet *et al.*, 2005). As such, this condition is not representative for the healthy brain. In healthy rodents, ABCC1 was found exclusively on brain capillaries but not astrocytes (Soontornmalai *et al.*, 2006). Our data presented here after ischaemia confirm these findings. In Western blots, we have never been able to detect ABCC1 in whole-brain homogenates (data not shown), but only in capillary-enriched fractions. We conclude that ABCC1 is not expressed in the brain parenchyma to relevant extent.

We did not observe ABCC2 expression on brain capillaries of FVB mice. The lack of ABCC2 expression is in line with

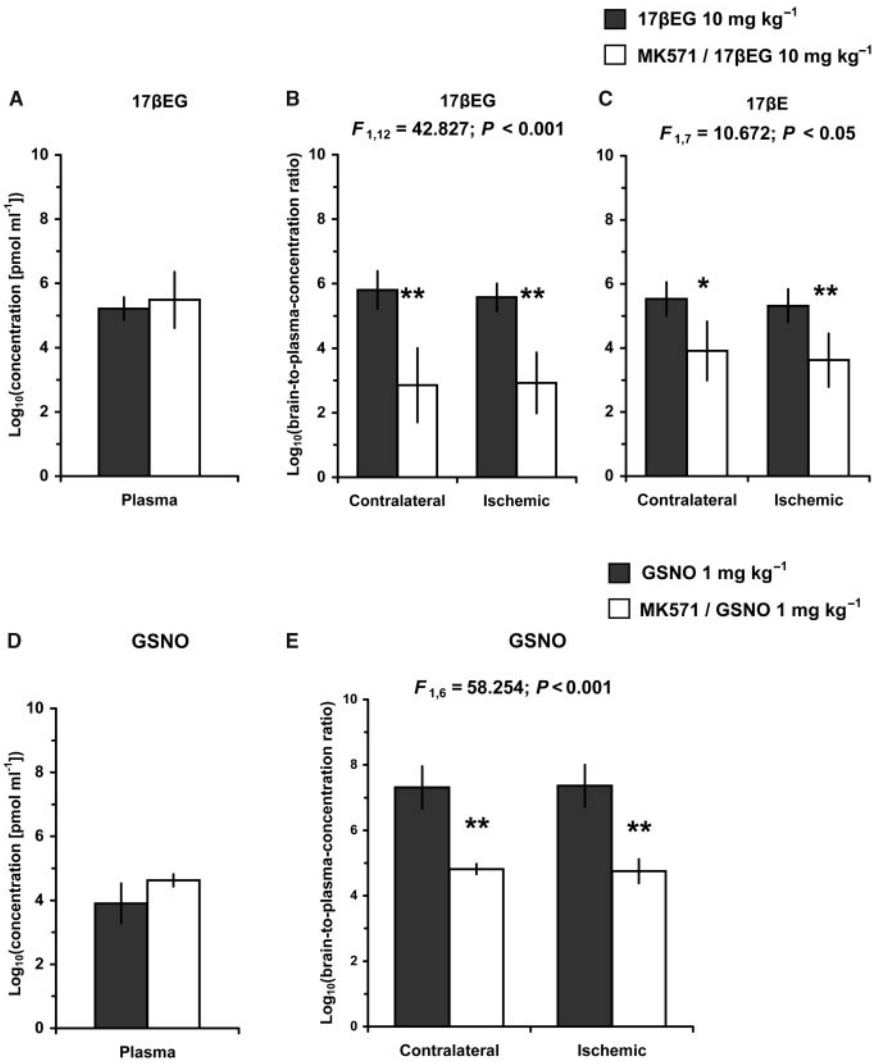

Fig. 4 Pharmacological inhibition of ABCC1 with MK571 dramatically reduces the brain accumulation of 17βEG and GSNO in C57Bl6/j mice. Plasma concentrations (**A** and **D**) and brain-to-plasma concentration ratios (**B, D** and **E**) for 17βEG, its parent 17βE and GSNO, analysed by LC-MS in mice submitted to focal cerebral ischaemia induced by 30 min MCA occlusion. Data are means ± SD [$n = 5$–7 per group (**A** and **B**), $n = 4$ per group (**C** and **D**)]. Repeated measurement ANOVA and *t*-tests (drug effects are shown). $^{*}P < 0.05$/$^{**}P < 0.01$ compared with animals receiving 17βEG (10 mg kg^{-1}) or GSNO (1 mg kg^{-1}) only.

previous studies, which also did not localize ABCC2 on brain capillaries in this mouse line (Soontornmalai *et al.*, 2006). As such, ABCC2's expression in FVB mice differs from C57Bl6/j mice (Soontornmalai *et al.*, 2006) and rats (van Vliet *et al.*, 2005), where ABCC2 expression was previously reported.

Choice of ABCC1 substrates

To evaluate the functionality of ABCC1, we chose two compounds, 17βEG and GSNO, which are known substrates of ABCC1 but not ABCB1 and which we considered both to be neuroprotective after stroke. In case of 17βE, survival-promoting actions are well established after focal cerebral ischaemia (Yang *et al.*, 2000; Rau *et al.*, 2003). In case of GSNO, neuroprotective effects had also been described in a rat model of ischaemic stroke (Khan *et al.*, 2005). We were surprised that GSNO exacerbated brain injury in mice after MCA occlusion. GSNO acts as NO donor, which promotes the reactivity of brain arterioles, but exacerbates neuronal injury via free radical formation (Dalkara and Moskowitz, 1994; Chan, 2001). Neuronal effects most likely explain the injury-aggravating effect of GSNO. Since we used 17βEG and GSNO as model compounds and were not interested in their mechanisms of action, the fact that GSNO increased ischaemic injury was of minor importance for our studies.

Considerations regarding earlier biodistribution studies

Previous reports had not been unambiguous about the role of ABCC1 in drug distribution. As such, an involvement of ABCC1 in drug elimination had been suggested following 17βEG and GSNO delivery in some (Nishino *et al.*, 1999;

Table 1 Tissue-to-plasma concentration ratios of 17βEG and 17βE in the liver, spleen and testis (in pmol mg^{-1} per pmol μl^{-1})

	17βEG			17βE		
	Liver	Spleen	Testis	Liver	Spleen	Testis
17βEG	6.01 ± 2.03	1.35 ± 0.45	0.60 ± 0.15	251.98 ± 134.40	19.46 ± 9.74	5.57 ± 2.11
MK571/17βEG	32.49 ± 25.90*	1.04 ± 0.25	0.89 ± 0.29*	810.00 ± 333.40*	23.66 ± 12.54	9.83 ± 5.28

*$P < 0.05$ compared with animals receiving 17βEG only (unpaired *t*-tests). $n = 7$ animals per group.

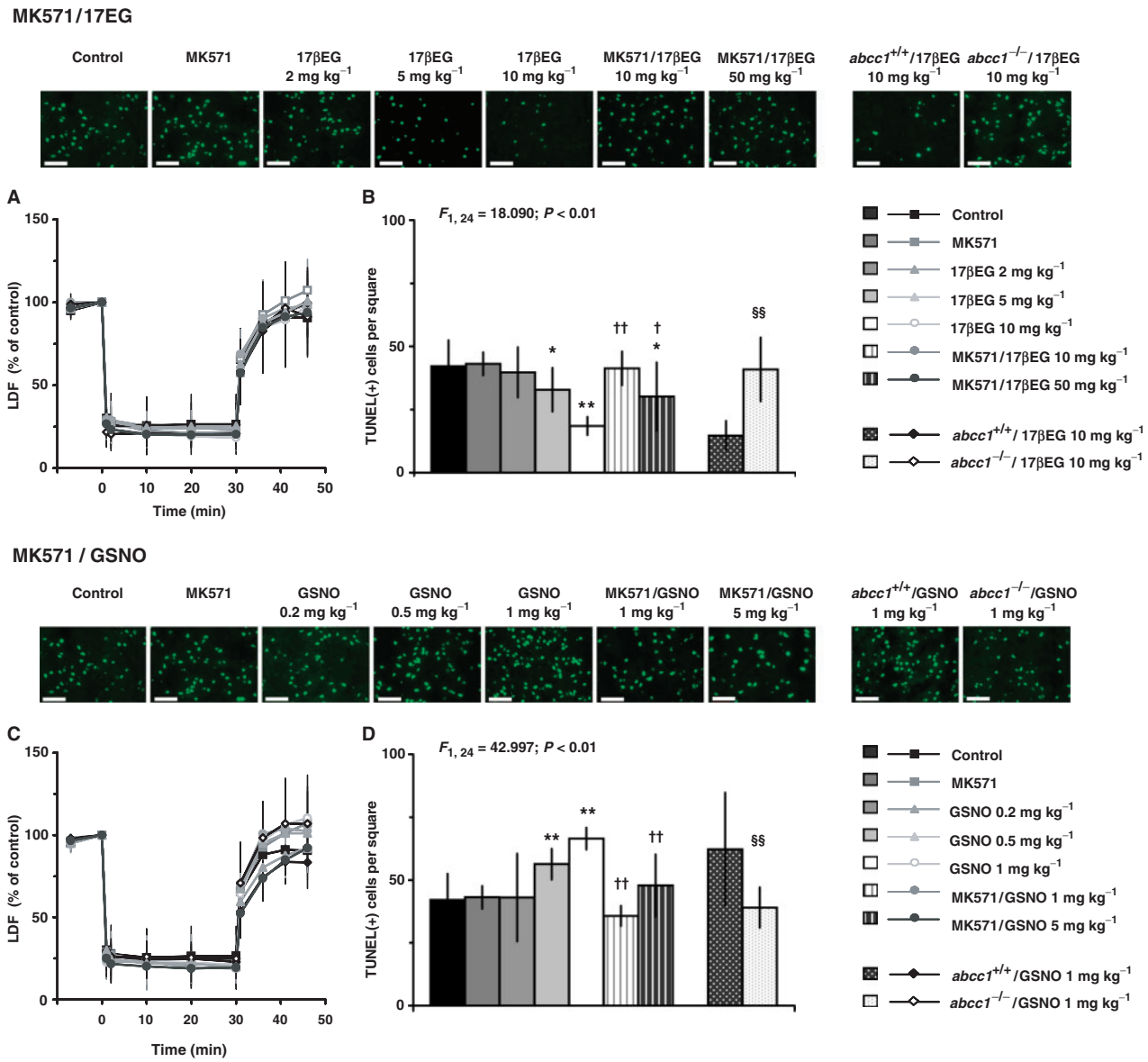

Fig. 5 Deactivation of ABCC1 abolishes 17βEG's neuroprotective and GSNO's neurotoxic effects after focal cerebral ischaemia induced by 30 min MCA occlusion. LDF measurements during and after ischaemia (**A** and **C**) and disseminate cell death evaluated by terminal transferase biotinylated-dUTP nick end labelling (TUNEL; green fluorescence) 72 h after reperfusion (**B** and **D**). Note the absence of blood flow changes between groups (**A** and **C**). Furthermore note that deactivation of ABCC1 by pharmacological blockade in C57Bl6/j mice and *abcc1*$^{-/-}$ in FVB mice almost completely reverses drug effects on ischaemic injury (**B** and **D**). Representative microphotographs for TUNEL stainings showing DNA-fragmented cells in the striatum are also presented. Data are means ± SD ($n = 7$–8 per group). One-way ANOVA and LSD tests (⩾3 groups), two-tailed *t*-tests (**B** and **D**: 2 groups), two-way ANOVA (**B** and **D**: 2 × 2 comparisons, drug interaction effects are shown). *$P < 0.05$/**$P < 0.01$ compared with vehicle-treated control mice; †$P < 0.05$/††$P < 0.01$ compared with animals receiving 17βEG (10 mg kg^{-1}) or GSNO (1 mg kg^{-1}) only; §§$P < 0.01$ compared with *abcc1*$^{+/+}$ mice. Bar = 120 μm.

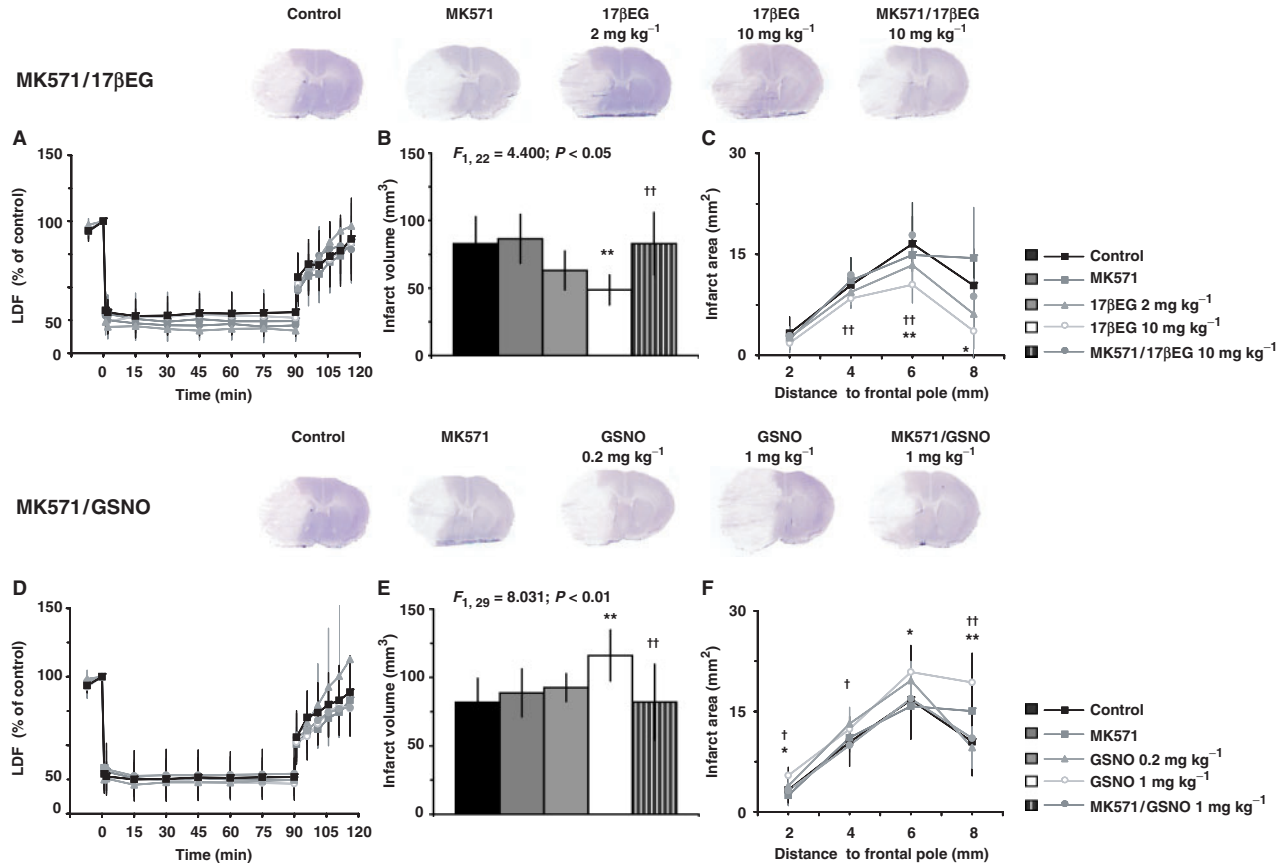

Fig. 6 Inhibition of ABCC1 with MK571 reverses 17βEG's neuroprotective and GSNO's neurotoxic effects after focal cerebral ischaemia induced by 90 min MCA occlusion. LDF during and after ischaemia (**A** and **D**), infarct volume (**B** and **E**) and infarct areas at various rostrocaudal brain levels (**C** and **F**) assessed by cresyl violet staining 24 h after reperfusion. Note again the absence of blood flow changes between groups (**A** and **D**). Note again that ABCC1 deactivation (here in C57Bl6/j animals) abolishes 17βEG's and GSNO's effects on infarct size (**B, C, E** and **F**). Data are means ± SD ($n = 6–8$ animals per group). One-way ANOVA and LSD tests (**A–F**), two-way ANOVA (**B** and **E**: 2 × 2 comparisons, drug interaction effects are shown). $^{*}P < 0.05/^{**}P < 0.01$ compared with vehicle-treated mice; $^{\dagger}P < 0.05/^{\dagger\dagger}P < 0.01$ compared with animals receiving 17βEG (10 mg kg^{-1}) or GSNO (1 mg kg^{-1}) only.

Sugiyama *et al.*, 2003), but not other (Cisternino *et al.*, 2003; Lee *et al.*, 2004) studies. Unfortunately, earlier studies strongly focused on ABCC1's role at the luminal endothelial membrane. As such, intra-cerebral (Sugiyama *et al.*, 2003) or intra-cerebroventricular (Nishino *et al.*, 1999; Lee *et al.*, 2004) drug infusions were mostly used. Moreover, autoradiographic techniques were applied for 17βEG and GSNO measurement (Nishino *et al.*, 1999; Cisternino *et al.*, 2003; Sugiyama *et al.*, 2003; Lee *et al.*, 2004), which did not distinguish 17βEG and GSNO from 17βE and glutathione, to which the molecules were cleaved (17βEG: shown here; GSNO: see Lee *et al.*, 2004). As a consequence, not the delivered parent compounds, but their metabolites were measured in the brain tissue. Methodological limitations explain the earlier non-specific findings.

Physiological role of ABCC1 at the BBB

The substrate affinity to glucuronidated, glutathionized and sulphated compounds is a characteristic feature of ABCC1 (Hermann and Bassetti, 2007). These compounds are so-called phase II degradation products, which have been metabolized in order to be excreted via the kidneys. The question arises to which purpose an ABC transporter accumulates conjugated molecules in the brain. Our observation that 17βEG uptake went along with elevated 17βE levels sheds light on this issue, indicating that 17βEG was deglucuronidated, most likely by β-glucuronidase (Brooks *et al.*, 2002). β-Glucuronidase is a lysosomal hydrolase constitutively expressed in the brain that is deficient in mucopolysaccharidosis VII (Brooks *et al.*, 2002), a neurodegenerative disorder. Our finding of 17βEG deglucuronidation suggests that ABCC1 enables 17βE recycling, offering the brain the possibility to regenerate conjugated molecules.

ABCC1 shares its affinity to phase II degradation products with transporters of the solute carrier-21 family, which are involved in drug uptake into capillary cells (Meier and Stieger, 2002; Hagenbuch and Meier, 2004). 17βEG and GSNO are known substrates of solute carrier-21 transporters, namely of organic anion transporter (Oatp)1a4, which is expressed at the luminal membrane of brain capillary

cells (Gao *et al.*, 1999). That ABCC1 accumulated drugs in the brain tissue implies that solute carriers were functional. The role of solute carriers in drug biodistribution will deserve additional attention in the future.

Implications of abluminal ABC transporters for drug development

That an active transporter contributes to drug accumulation in the brain following stroke has important clinical implications. As such, the brain access of drugs may markedly be improved by chemical modifications resulting in increased ABCC1 affinity. In view of ABCC1's strong affinity to conjugated molecules, glucuronidation, glutathionization or sulphatation may render drugs able to pass the BBB. Drug–protein interactions have gained huge interest in drug development recently. As such, crystal structures have offered new insights into the kinetics of drug binding with ABC transporters (Murakami *et al.*, 2006). Based on our data, crystal structures might allow the selection of new generations of drugs that bind to abluminal, but lack interactions with luminal ABC transporters. This might potently increase brain accumulation and drug efficacy, and enhance the overall success of pharmacological therapies.

Supplementary material

Supplementary material is available at *Brain* online.

Acknowledgements

We thank Ursula Gutteck-Amsler, Angela Fendel, Maja Günthert and Areejittra Soontornmalai for technical assistance.

Funding

Swiss National Center of Competence in Research 'Neural plasticity'; the Swiss National Science Foundation (3200B0-112056/1); Baasch-Medicus Foundation; Hermann-Klaus Foundation; David-and-Betty-Koetser Foundation (to D.M.H.).

References

Begley DJ. Delivery of therapeutic agents to the central nervous system: the problems and the possibilities. Pharmacol Ther 2004; 104: 29–45.

Berezowski V, Landry C, Dehouck MP, Cechelli R, Fenart L. Contribution of glial cells and pericytes to the mRNA profiles of p-glycoprotein and multidrug resistance-associated proteins in an in vitro model of the blood-brain barrier. Brain Res 2004; 1018: 1–9.

Brooks AI, Stein CS, Hughes SM, Heth J, McCray PM, Sauter SL, et al. Functional correction of established central nervous system deficits in an animal model of lysosomal storage disease with feline immunodeficiency virus-based vectors. Proc Natl Acad Sci USA 2002; 99: 6216–21.

Chan PH. Reactive oxygen radicals in signaling and damage in the ischemic brain. J Cereb Blood Flow Metab 2001; 21: 2–14.

Cisternino S, Rousselle C, Lorico A, Rappa G, Scherrmann JM. Apparent lack of Mrp1-mediated efflux at the luminal side of mouse blood-brain barrier endothelial cells. Pharm Res 2003; 20: 904–9.

Dalkara T, Moskowitz MA. The complex role of nitric oxide in the pathophysiology of focal cerebral ischemia. Brain Pathol 1994; 4: 49–57.

Dombrowski SM, Desai SY, Marroni M, Cucullo L, Goodrich K, Bingaman W, et al. Overexpression of multiple drug resistance genes in endothelial cells from patients with refractory epilepsy. Epilepsia 2001; 42: 1501–6.

Gao B, Stieger B, Noé B, Fritschy J-M, Meier PJ. Localization of the organic anion transporting polypeptide 2 (Oatp2) in capillary endothelium and choroids plexus epithelium of rat brain. J Histochem Cytochem 1999; 47: 1255–63.

Hagenbuch B, Meier PJ. Organic anion transporting polypeptides of the OATP/SLC21 family: phylogenetic classification as OATP/SLCO superfamily, new nomenclature and molecular/functional properties. Pflugers Arch 2004; 447: 653–65.

Hermann DM, Bassetti CL. Implications of ATP-binding cassette transporters for brain pharmacotherapies. Trends Pharmacol Sci 2007; 28: 128–34.

Hermann DM, Kilic E, Spudich A, Krämer SD, Wunderli-Allenspach H, Bassetti CL. Role of drug efflux carriers in the healthy and diseased brain. Ann Neurol 2006; 60: 489–98.

Higgins CF, Hiles ID, Salmond GP, Gill DR, Downie JA, Evans IJ, et al. A family of related ATP-binding subunits coupled to many distinct biological processes in bacteria. Nature 1986; 323: 448–50.

Khan M, Sekhon B, Giri S, Jatana M, Gilg AG, Ayasolla K, et al. S-Nitrosoglutathione reduces inflammation and protects brain against focal cerebral ischemia in a rat model of experimental stroke. J Cereb Blood Flow Metab 2005; 25: 177–92.

Kilic E, Kilic Ü, Wang Y, Bassetti CL, Marti HH, Hermann DM. The phosphatidylinositol-3 kinase/Akt pathway mediates VEGF's neuroprotective activity and induces blood brain barrier permeability after focal cerebral ischemia. FASEB J 2006; 20: 1185–7.

Kimura A, Ishida Y, Wada T, Yokoyama H, Mukaida N, Kondo T. MRP-1 expression levels determine strain-specific susceptibility to sodium arsenic-induced renal injury between C57BL/6 and BALB/c mice. Toxicol Appl Pharmacol 2005; 203: 53–61.

Lee YJ, Kusuhara H, Sugiyama Y. Do multidrug resistance-associated protein-1 and -2 play any role in the elimination of estradiol-17 beta-glucuronide and 2,4-dinitrophenyl-S-glutathione across the blood-cerebrospinal fluid barrier? J Pharm Sci 2004; 93: 99–107.

Löscher W, Potschka H. Drug resistance in brain diseases and the role of drug efflux transporters. Nat Rev Neurosci 2005; 6: 591–602.

Meier PJ, Stieger B. Bile salt transporters. Annu Rev Physiol 2002; 64: 635–61.

Mueller CFH, Widder JD, McNally JS, McCann L, Jones DP, Harrison DG. The role of multidrug resistance protein-1 in modulation of endothelial cell oxidative stress. Circ Res 2005; 97: 637–44.

Murakami S, Nakashima R, Yamashita E, Matsumoto T, Yamaguchi A. Crystal structures of a multidrug transporter reveal a functionally rotating mechanism. Nature 2006; 443: 173–9.

Nishino J, Suzuki H, Sugiyama D, Kitazawa T, Ito K, Hanano M, et al. Transepithelial transport of organic anions across the choroid plexus: possible involvement of organic anion transporter and multidrug resistance-associated protein. J Pharmacol Exp Ther 1999; 290: 289–94.

O'Collins VE, Macleod MR, Donnan GA, Horky LL, van der Worp BH, Howells DW. 1,026 experimental treatments in acute stroke. Ann Neurol 2006; 59: 467–77.

Pardridge WM. Drug and gene delivery to the brain: the vascular route. Neuron 2002; 36: 555–8.

Rau SW, Dubal DB, Böttner M, Gerhold LM, Wise PM. Estradiol attenuates programmed cell death after stroke-like injury. J Neurosci 2003; 23: 11420–6.

Regina A, Koman A, Piciotti M, El Hafny B, Center MS, Bergmann R, et al. Mrp1 multidrug resistance-associated protein and p-glycoprotein expression in rat brain microvessel endothelial cells. J Neurochem 1998; 71: 705–15.

Rizzi M, Caccia S, Guiso G, Richichi C, Gorter JA, Aronica E, et al. Limbic seizures induce P-glycoprotein in rodent brain: functional implications for pharmacoresistance. J Neurosci 2002; 22: 5833–9.

Seetharaman S, Barrand MA, Maskell L, Scheper RJ. Multidrug resistance-related transport proteins in isolated human brain microvessels and in cells cultured from these isolates. J Neurochem 1998; 70: 1151–9.

Soontornmalai A, Vlaming ML, Fritschy J-M. Differential, strain-specific cellular and subcellular distribution of multidrug transporters in murine choroid plexus and blood-brain barrier. Neuroscience 2006; 138: 159–69.

Spudich A, Kilic E, Xing H, Kilic Ü, Rentsch KM, Wunderli-Allenspach H, et al. Inhibition of multidrug resistance transporter-1 facilitates neuroprotective therapies after focal cerebral ischemia. Nat Neurosci 2006; 9: 487–8.

Sugiyama D, Kusuhara H, Lee Y-J, Sugiyama Y. Involvement of multidrug resistance associated protein 1 (Mrp1) in the efflux transport of 17beta estradiol-D-17beta-glucuronide (E217betaG) across the blood-brain barrier. Pharm Res 2003; 20: 1394–400.

van Vliet EA, Redeker S, Aronica E, Edelbroek PM, Gorter JA. Expression of multidrug transporters MRP1, MRP2, and BRCP shortly after status epilepticus, during the latent period, and in chronic epileptic rats. Epilepsia 2005; 46: 1569–80.

Wang Y, Kilic E, Kilic Ü, Weber B, Bassetti CL, Marti HH, et al. VEGF overexpression induces post-ischaemic neuroprotection, but facilitates haemodynamic steal phenomena. Brain 2005; 128: 52–63.

Yang SH, Shi J, Day AL, Simpkins JW. Estradiol exerts neuroprotective effects when administered after ischemic insult. Stroke 2000; 31: 745–9.